atmosphere

MDPI

Article

Observational and Modelling Study of a Major Downburst Event in Liguria: The 14 October 2016 Case

Antonio Parodi [1,*], Martina Lagasio [1], Maurizio Maugeri [2], Barbara Turato [3] and William Gallus [4]

1 International Centre on Environmental Monitoring (CIMA), Research Foundation, 17100 Savona, Italy; martina.lagasio@cimafoundation.org
2 Department of Environmental Science and Policy, Università degli Studi di Milano, 20122 Milano MI, Italy; maurizio.maugeri@mi.infn.it
3 ARPAL—Ligurian Regional Environmental Protection Agency, 16149 Genova GE, Italy; barbara.turato@arpal.gov.it
4 Geological and Atmospheric Sciences, Iowa State University, Ames, IA 50011, USA; wgallus@iastate.edu
* Correspondence: antonio.parodi@cimafoundation.org

Received: 3 November 2019; Accepted: 3 December 2019; Published: 6 December 2019

Abstract: Downbursts are very disruptive weather events that can produce large amounts of damage. The most studied downbursts are those occurring in the United States and continental Europe, but they can happen globally. This work is an observational and modelling analysis of a major downburst event that occurred on 14 October 2016 over eastern Liguria (Italy). This downburst affected an area 30 km long and 10 km wide, producing observed wind gusts of 40 m/s with major impacts to railways, trees, and houses, with more than 2.5 million euros of damage. First, the general environment influencing this downburst is identified and analyzed, then the event is reproduced with a small multi-physics high-resolution ensemble using the Weather Research and Forecasting (WRF)–advanced research WRF (ARW) model, with 1 km horizontal grid spacing. The event was poorly predicted beforehand, and the difficulty in forecasting this event is confirmed by the fact that so few ensemble members suggested the occurrence of damaging winds over eastern Liguria. However, one of the eight members performed well and its output helped to reveal the primary mechanisms for the downburst, suggesting that high-resolution ensembles using mixed physics may be a useful tool for improving the prediction of similar extreme events in the Mediterranean region in the future.

Keywords: downburst; WRF-ARW; predictability

1. Introduction

Downbursts are among the most disruptive severe weather events, with large socio-economic impacts. Downbursts occur globally, although traditionally those in the United States and continental Europe have been studied most thoroughly. In a sequence of seminal papers, Fujita studied these phenomena in terms of their spatial–temporal scales and related meteorological characteristics [1–3]. Fujita postulated the existence of the downburst as a strong downdraft, which induces an outburst of damaging winds on or near the ground. These damaging winds, either straight or curved, are highly divergent. In preparation for the Northern Illinois Meteorological Research on Downbursts (NIMROD) project, [1] identified two particular radar cell types as especially significant for the production of downbursts: The hook echo, which was already well associated with supercell storms and tornadoes, and a bow-shaped line of cells, which is now commonly defined as a bow echo. Fujita also coined

the term microburst for downbursts smaller than 4 km, and macroburst for downbursts larger than 4 km [4].

Many downburst observational studies focused on events in the continental United States [5–10], with some others studying events in India [11], Australia [12], and Europe [13–16]. Using numerical modelling, [17] simulated an idealized downburst-producing thunderstorm with cloud permitting grid spacing (2 km) using the RAMS (Regional Atmospheric Modelling System), strongly suggesting that simplified models, such as the impinging jet and cooling source models, are not sufficient for capturing the spatial and temporal nature of near-surface flow found in downburst-producing thunderstorms. Along similar lines, [18] showed how high-resolution numerical modelling, down to kilometer horizontal grid spacing, can support the prediction of thermodynamic ingredients leading to the occurrence of microbursts.

The number of observational and modelling studies of downbursts in the Mediterranean region is low despite the fact that this area represents a hot spot from a climate change standpoint for severe hydro-meteorological events. [19] studied the environment of the downbursts on 21 June 1984 and 9 September 1992, both in Menorca (Balearic Islands). More recently, [16] studied a downburst episode in Livorno (central Italy) that occurred on 1 October 2012 on a spatial scale of 2–3 km, by using model analyses, standard in situ measurements, remote sensing techniques, proxy data, and direct observations. Their results brought new insights into a downburst's predictability in the Mediterranean, its evolution at the local scale, and the possible role of specific synoptic-scale weather conditions, like secondary cyclogenesis in the lee of the Alps.

The present paper is an observational and modelling study of a large downburst, or macroburst, episode that occurred on 14 October 2016 over eastern Liguria. To the best of the authors' knowledge, and on the basis of a thorough review of scientific papers and newspapers dating back to the early decades of the twentieth century, this is the first major downburst episode ever observed and studied over the Liguria area. Prior to the event, forecasters noted that the meteorological scenario was favorable enough for the issuing of a maximum (red) level of alert by the Ligurian Regional Environmental Protection Agency (ARPAL), for the possible development of an organized and quasi-stationary heavily precipitating convective system in the Gulf of Genoa, a relatively common scenario [20,21] often producing major flash-floods. Gusty winds around 20–25 m/s were also expected.

Somewhat unexpectedly, a long convective line developed over the southwestern part of the Ligurian Sea and quickly evolved into a severe bow-echo system rapidly propagating downwind towards the Liguria region. As soon as the bow-echo reached the coast, a macroburst developed with an intense gust front and cold pool: Wind gusts up to 40 m/s were observed over an area 30 km long and 10 km wide, with major impacts on railways, trees, and houses, and economic damage of more than 2.5 million euros. At the same time, temperatures rapidly dropped by about 10 °C in a few tens of minutes.

Different data sources, such as radar, in situ weather station, and lightning sensors, will be used to reconstruct the observed spatial–temporal evolution of the macroburst, and to validate modelling results obtained with multi-physics Weather Research and Forecasting (WRF) simulations using horizontal grid spacing as fine as 1 km. Concerning the radar data, the C-band Settepani radar managed by ARPAL (Liguria Region) and well located for this downburst event was down for technical problems. Thus, only data (Vertical Max Reflectivity) from the Collobrieres radar (MeteoFrance) were available).

Section 2 describes the WRF model setup and the multi-physics ensemble rationale. Section 3 describes the synoptic and mesoscale environment of the event. Section 4 presents and discusses the research results. Finally, Section 5 draws conclusions and discusses operational implications.

2. WRF Model Setup

The WRF model, version 3.8 with the advanced research WRF (ARW) dynamic core is a fully compressible and nonhydrostatic regional atmospheric model, with terrain following hydrostatic

pressure vertical coordinates [22]. The WRF domain setup for this case study is based on the modelling results achieved for two other extreme autumn events that happened in the Liguria Region in November 2011 [23], and October 2014 [20,24]. Two nested domains with, respectively, 5 km (179 × 200 grid points) and 1 km (475 × 475 grid points) horizontal grid spacing were used to cover the upper and lower limits of the cloud-permitting range [25]. The number of vertical levels over the 20 km atmosphere depth is equal to 83 (lowest model level at 50 m and 10 model levels in the first 1000 m) since the sensitivity analysis performed in [23] demonstrated the importance of fine grid spacing also in the vertical direction. All of the analyses presented hereafter refer to the innermost domain with 1 km grid spacing.

The multi-physics experiments focus on the combination of four different microphysics parameterizations with two different planetary boundary layer schemes:

- The WRF single-moment six-class (WSM6) scheme with graupel [26];
- The Thompson six-class scheme including graupel with ice and rain number concentrations also predicted [27];
- The WRF double-moment six-class (WDM6) scheme [28], which is the version of WSM6 that is double-moment for warm rain processes, with cloud condensation nuclei (CCN), and number concentrations of cloud and rain predicted;
- The Morrison double-moment six-class scheme [29], with number concentrations also predicted for ice, snow, rain, and graupel.

The adopted microphysics schemes allowed an exploration of the uncertainty in predicting the key microphysical processes, such as rain evaporation and graupel/hail melting, for the severe weather event under consideration.

The planetary boundary layer (PBL) parameterizations used were the Yonsei University (YSU) [30] and the Mellor–Yamada–Janjic (MYJ) [31]. YSU is a non-local scheme with a top-down mixing option for turbulence driven by cloud-top radiative cooling which is separate from bottom-up surface-flux-driven mixing. MYJ is a 1.5-order, level 2.5, turbulence kinetic energy (TKE) prediction-based scheme, with local TKE-based vertical mixing in the boundary layer and free atmosphere. A large eddy simulation (LES)-like turbulence closure was adopted [32]. The Rapid Update Cycle (RUC) land surface model was chosen: it predicts soil temperature and soil moisture in six layers.

The RRTMG shortwave and longwave scheme, a spectral scheme with 16 longwave bands and 14 shortwave bands, was used [33]. It adopts look-up table fits to accurate calculations, and it can interact with trace gases and aerosols.

All of the modelling experiments were driven by initial and boundary conditions provided by the European Centre for Medium-Range Weather Forecasts Integrated Forecast System with a spatial resolution of 0.125° × 0.125°. All eight simulations were initialized at 00 UTC on 14 October 2016, roughly 12 h before the main downburst event, and the lateral boundaries were updated every 3 h.

3. Synoptic and Mesoscale Environment

The analyzed event occurred in a synoptic environment typical of those that produce substantial convective systems, often with heavy rainfall, near Liguria [23]. According to the ECMWF (European Centre for Medium-Range Weather Forecasts)-ERA5 (ECMWF Re-Analysis) reanalysis [34], at 06 UTC 14 October (Figure 1), a wide baroclinic trough extended from the northwestern Atlantic to the western Mediterranean, with the main axis southeasterly oriented near the border of France and Spain, and a cut-off low at 500 hPa moving eastward. This pattern produced strong south to southwesterly flow in the mid tropospheric levels over the Liguria region, ahead of the trough axis.

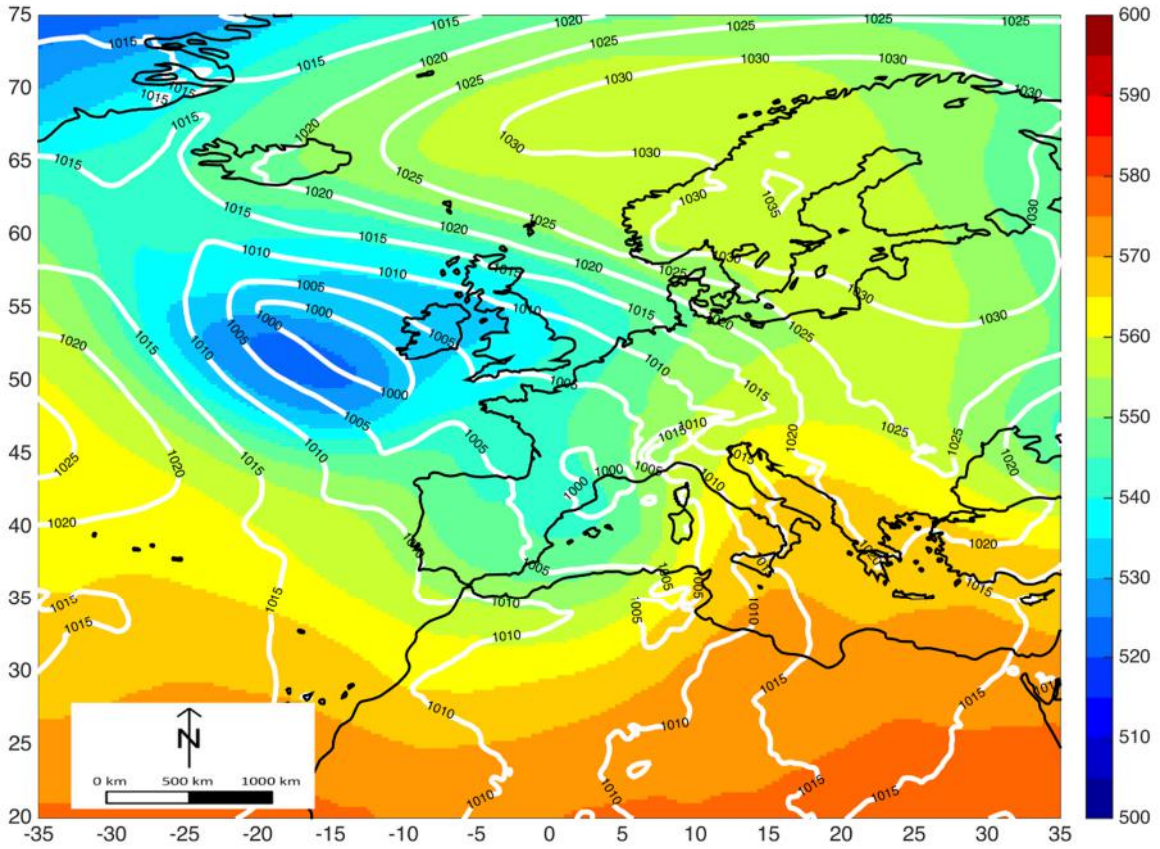

Figure 1. Geopotential heights (shaded according to color bar on the right of the figure) at 500 hPa and mean sea level pressure (white, contour interval 5 hPa) at 06 UTC on 14 October 2016 (ECMWF-ERA5).

At the surface, a wide low-pressure system affected western Europe with two low pressure centers. The main cyclone, in its mature phase, was centered just west of Ireland, well aligned with the cut-off low aloft. The secondary cyclone, of orographic lee origin, as found in the downburst case studied by [16], and relatively stationary, was located in the Gulf of Lion (in the lee of the Pyrenees). Its position was favorable to establish a strong warm and moist flow from southern latitudes towards Liguria. In this regard, it is interesting to note that the surface temperatures on 14 October, recorded at 06 UTC, reached values of 20 to 24 °C in Corsica, Sardinia, and the southeastern regions of France (Figure 2), while temperatures in the western and central parts of the Liguria region reached only 14 to 16 °C (06 UTC, Figure 2a,b), highlighting that the warm flux did not reach that area.

In fact, due to the presence of a mesoscale region of higher pressure across the Po Plain (Figure 1), an intense flow of cool air funneled southward through the lower gaps in the northern Apennines. It produced strong northerly winds in the western part of Liguria in the 12 h before the event (with maximum values of roughly 20 m/s), which resulted in about two degrees of cooling in this area between 06 and 09 UTC (Figure 2).

ASCAT (Advanced Scatterometer) winds for this case around 09 UTC (Figure 3) show a convergence zone between Liguria and Corsica, from around 9 E longitude near the coast arcing toward the southwest. This convergence line was associated with a strong stationary thermal boundary, where the warm and moist air flowing through the Tyrrhenian Sea met the relatively cold air coming south out from the Po Valley. During the morning, the thermal boundary became the initiation mechanism for convective structures, which tried to evolve into more organized systems (9–10 UTC). Nevertheless, due to the high values of low-level wind shear (not shown), the convection did not evolve into a quasi-stationary or back-building MCS, and instead cells were driven towards the Ligurian coast. Figure 3 also shows another stationary convergence line extending from southeastern France to Corsica, in association

with the quick propagation of a shortwave trough. It is important to note that some signs of strong low-level winds and a developing cold pool could be seen on the northwestern coast of Corsica in the late morning. The surface observation (METAR) data at the Calvi station (LFKC) recorded a maximum wind gust of 38 m/s (mean wind over 10 min period equal to 9 m/s) at 830 UTC with a pressure change of 7 hPa (increasing from 1001 to 1008 hPa) and a temperature decrease of 8 °C from 8 to 9 UTC. Further north, the SYNOP/BUFR data at Cap Corse indicated a maximum wind gust of 37.5 m/s half an hour later (at 9 UTC, the mean wind over 10 min was 16.5 m/s), a pressure change of 4 hPa (increasing from 1002.6 to 1006.1 hPa from 9 to 11 UTC) and a temperature decrease of about 6 °C from 10 to 11 UTC. These observations support the idea that the strong windstorm likely developed far from Liguria and occurred on a wide spatial scale.

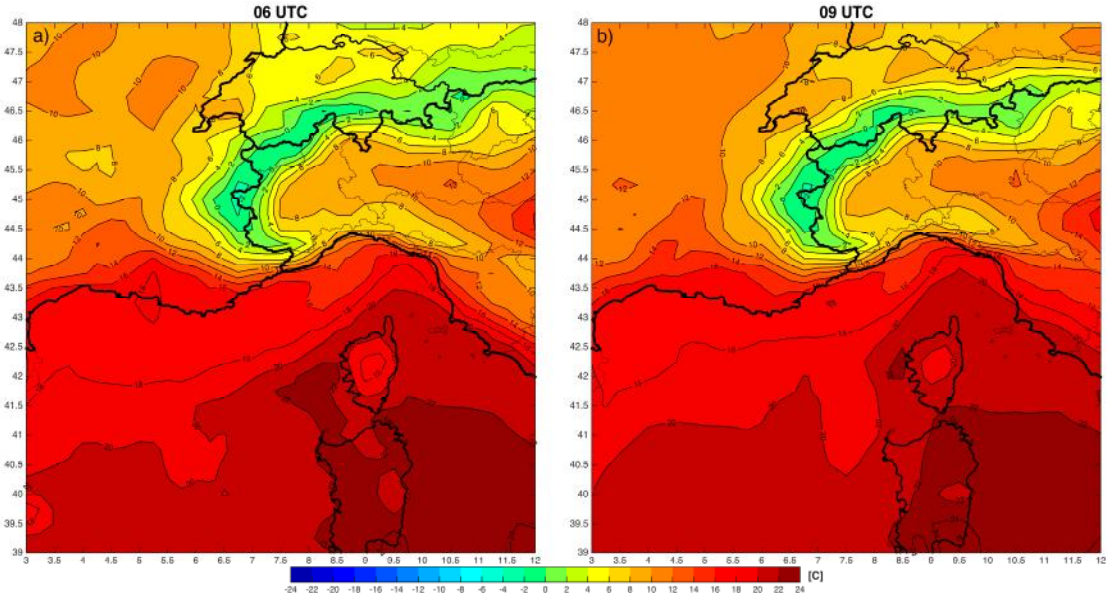

Figure 2. ECMWF-ERA5 reanalysis temperatures at 06 UTC (**a**) and 09 UTC (**b**) over the western Mediterranean and western Europe.

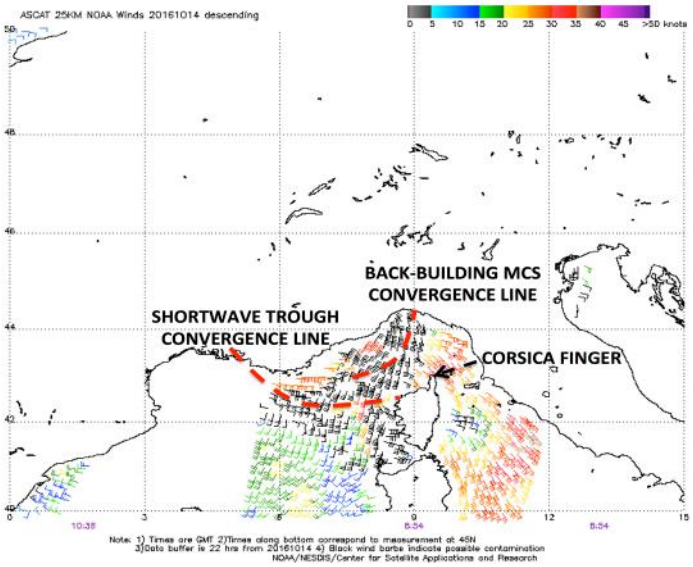

Figure 3. ASCAT winds (full barb is 5 kts) at 09 UTC on 14 October 2016. Calvi and Corsica finger positions are highlighted.

Around 1020 UTC, the eastern part of the convergence line, associated with the shortwave trough and elongated from southern France to the Corsica "finger" (the northern peninsula, Figure 4) showed a small area of acceleration forming a bow echo structure in the radar data, emerging on the eastern flank of Corsica. The bow-shaped convective line rapidly propagated north-eastward in the direction of the mean low-level vertical wind shear vector and spread out. It covered a distance of about 150 km in about 1 h and 45 min, reaching the Liguria coast around 1130 UTC. The weak echo notch behind the bow is well aligned with the typical location of a strong descending rear-inflow jet (e.g., [35,36]).

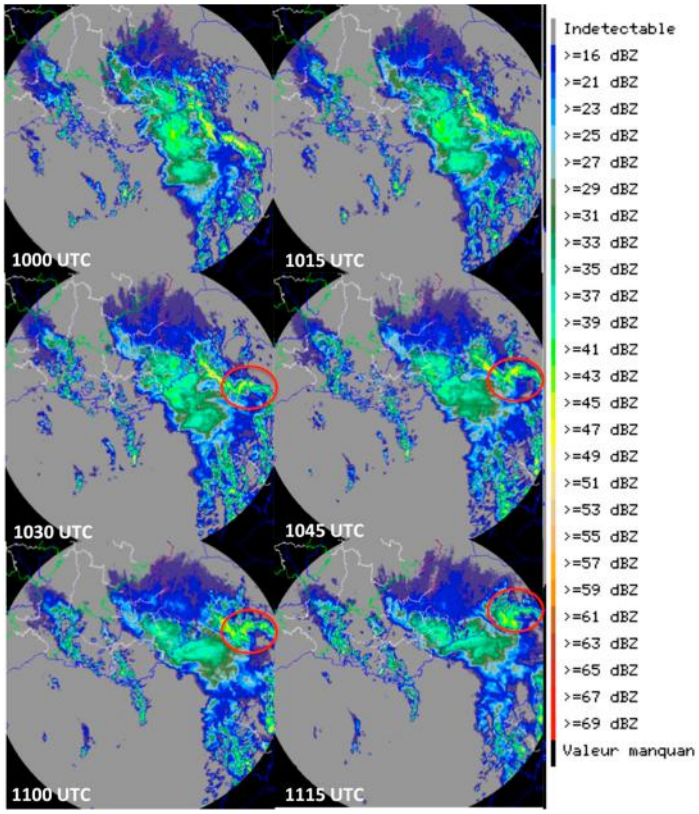

Figure 4. Radar reflectivity from the Collobrieres radar (MeteoFrance) from 1000 UTC to 1115 UTC on 14 October 2016. The red ellipse highlights the position of the bow echo structure developing near northern Corsica.

The resulting macroburst had a longitudinal extent of about 60 km, with widespread largest impacts from Sant'Ilario to Chiavari (Figure 5), including extensive damage to trees, the local railway network, and roofs of houses, among other things.

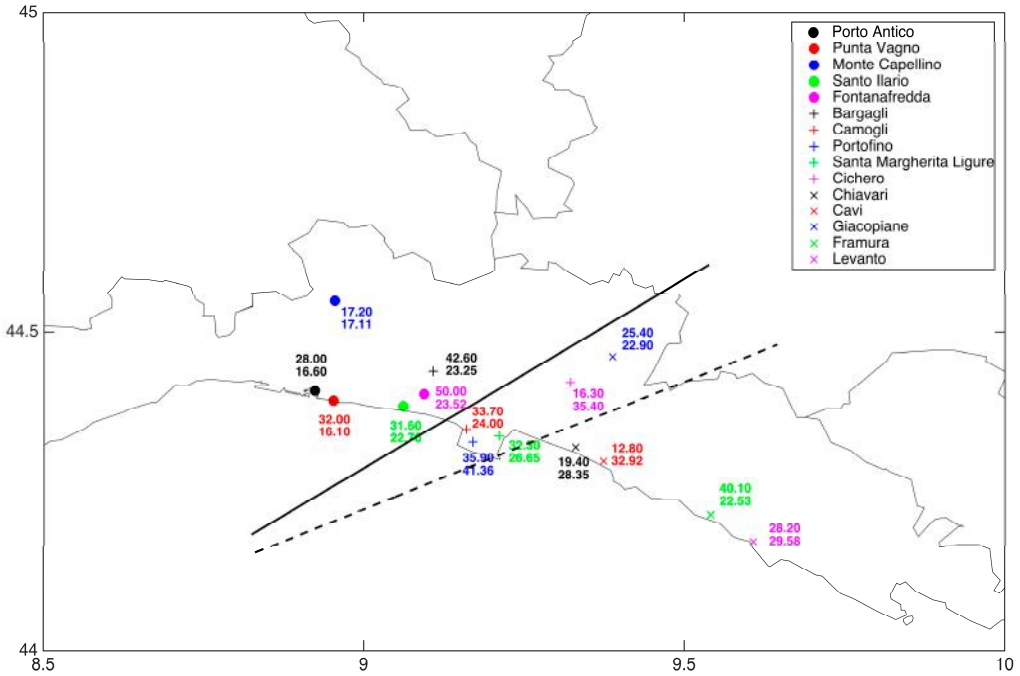

Figure 5. Region affected by the downburst from Porto Antico station (black bullet marker) to Levanto station (red cross marker) for about 65 km. For each marker, the upper number represents the maximum observed wind gust, while the lower number represents the maximum predicted wind gust by the ensemble runs, over the time interval 11–13 UTC. Continuous line shows the main axis orientation of the observed downburst, while the dashed one corresponds to ensemble predicted downburst.

4. Results

First, the multi-physics ensemble modeling results are explored by comparing the observed and predicted 10 m wind speed at 15 ARPAL station locations, which cover the entire area affected by the macroburst. These stations provide the maximum wind intensity and average wind observations (at 10 m) in 10 min intervals, while WRF output is available with 5 min temporal resolution. The results in Figure 5, in combination with the comparison of observed maximum wind speed and maximum value predicted by any of the ensemble members at the station locations (Figure 6), suggest that over the whole region generally affected by the downburst, along the coastline from Porto Antico to Levanto and inland up the hills to Giacopiane, the observed and ensemble predicted values are comparable with peak values of up to 40–50 m/s. It is worth mentioning here that only one of the experiments predicted peak values of up 40–50 m/s, with the other ones significantly lower, almost 20% below the peak observed values. Furthermore, the ensemble predicted wind gust values suggest that the predicted macroburst is more aligned towards the eastern side of Liguria, while the observed one affected mostly central Liguria (on the western side of the Portofino promontory), with an overall error in location on the order of 10–15 km.

Concerning the 2 m temperature field (Figure 7), limited to the three coastal stations belonging to the innermost area spanned by the predicted and observed macroburst, all ensemble members satisfactorily capture the observed temporal evolution with the initial 4–5 K temperature increase (8–12 UTC), due primarily to the warm advection from the strong southerly surface flow induced by the shortwave trough aloft. Moreover, they successfully describe the subsequent and sudden temperature decrease (up to 8–9 °C in 30 min) once the macroburst has formed and propagated towards the Liguria coastline. Of note, at the Portofino station location, a temperature warm bias is apparent in the modeling results with respect to observations, but this is probably due to WRF model local topography interpolation errors.

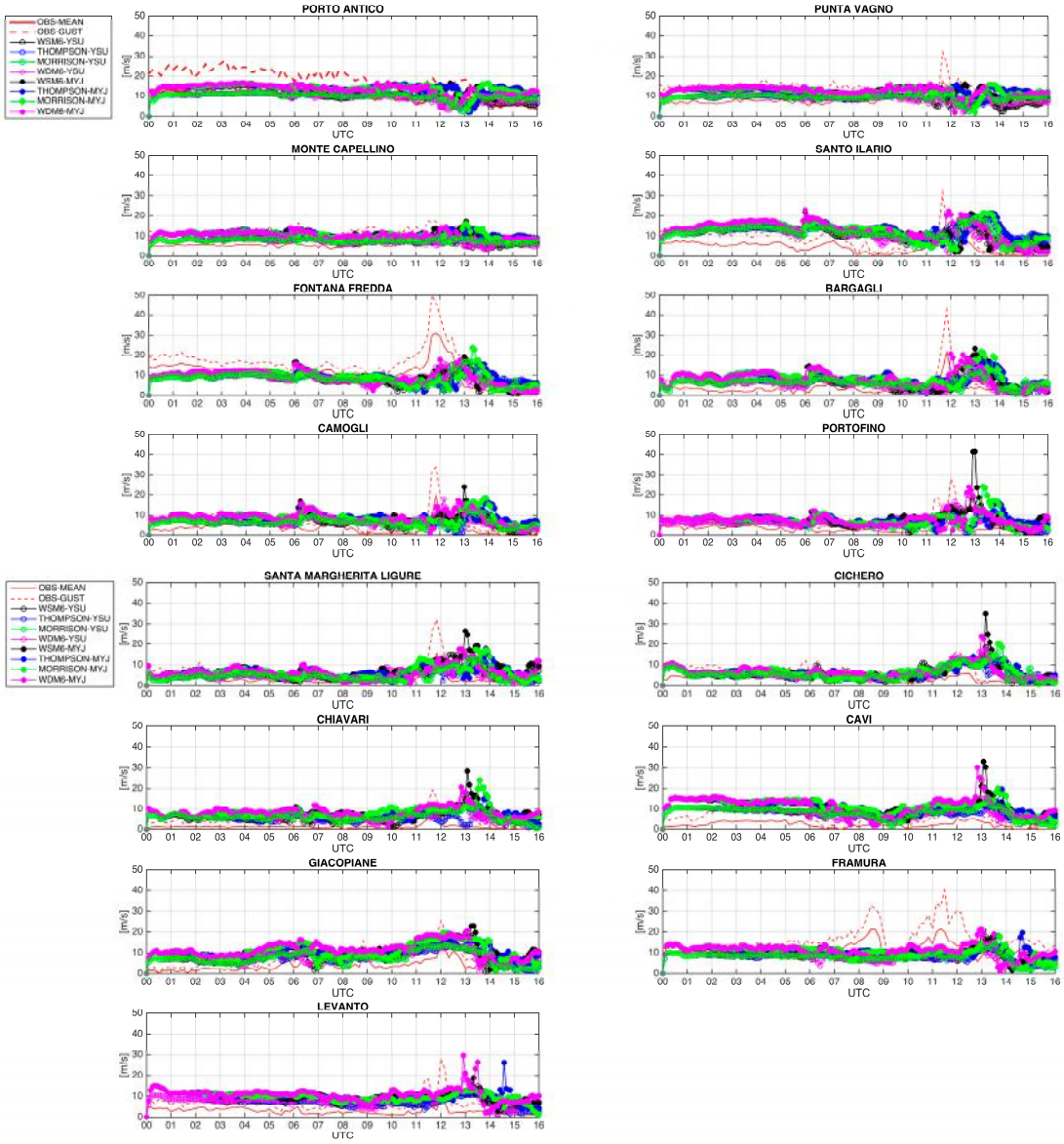

Figure 6. Comparison between observed and ensemble predicted wind gust for the period 00–18 UTC at the 15 ARPAL stations locations. Each subplot refers to different wind station locations in Liguria.

Shifting the focus to the behavior of the individual ensemble members, the 10 min wind speeds (Figure 6) show that the best performing WRF setup uses the WSM6 microphysics in combination with the MYJ PBL scheme. This member is able to produce a peak wind speed around 41 m/s at Portofino's location (13 UTC); this value is in good agreement with the wind maximum of 50 m/s observed at Fontanafredda (1145 UTC), with a spatial displacement error of only 10–15 km and a timing error around 1 h.

This good performance suggests that the WSM6-MYJ simulation is able to capture the key observed ingredients associated with the generation and propagation of the macroburst. Conversely the other ensemble members do not correctly predict the key ingredients of the observed severe wind scenario, and among them, the Thompson-YSU simulation is the worst performing, with wind speed peaks in any 5 min period lower than 10 m/s at or near the selected locations.

Indeed, the WSM6-MYJ simulation shows, at 950 hPa, a coherent cold pool structure characterized by a temperature change over time up to −4 °C/1 h, propagating from western Corsica to the Liguria Sea Gulf (Figure 8, left column) along the direction of the 0–3 km shear: The cold pool propagation

speed is estimated at around 23 m/s. A similar structure is present in the Thompson-YSU simulation (Figure 8, right column), but with a somewhat narrower region of strong cooling and a less pronounced bowing structure by 13 UTC.

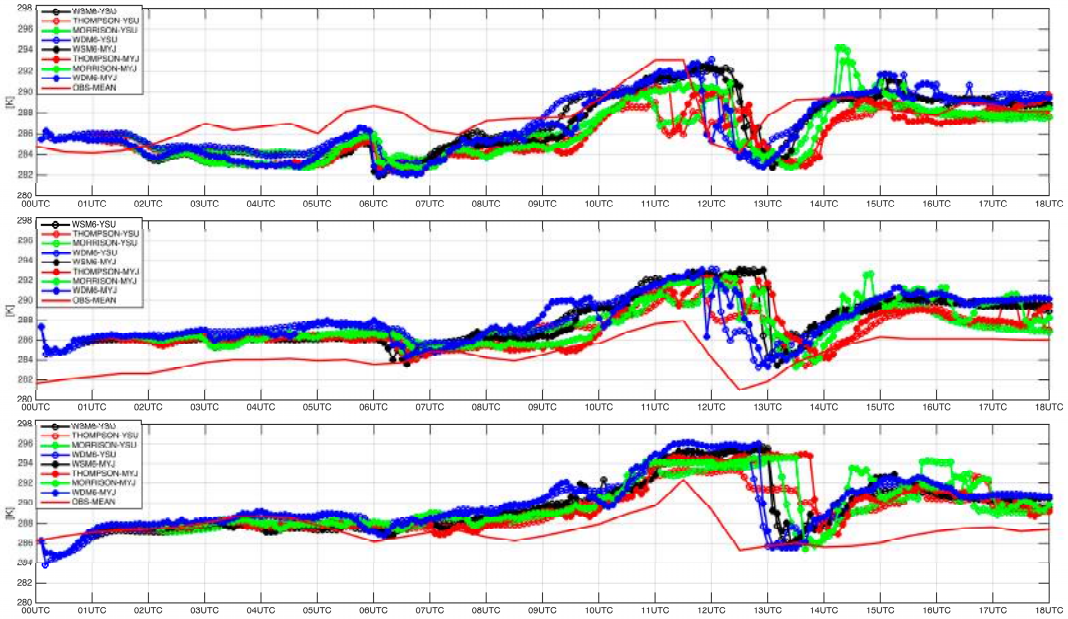

Figure 7. Comparison between observed and predicted 2 m temperatures for the period 00–18 UTC at Sant'Ilario, Portofino, and Chiavari (panels from top to bottom).

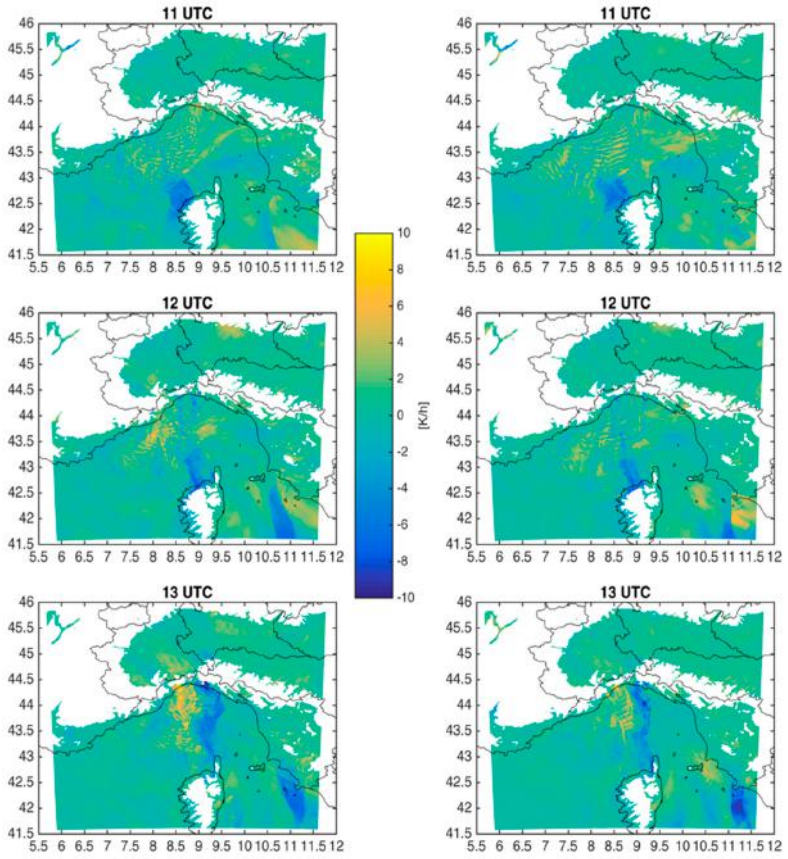

Figure 8. The 950 hPa temperature tendency for the previous 1 h at 11, 12, and 13 UTC (WSM6-MYJ, left column; Thompson-YSU, right column).

In the area of the cold pool it is possible to identify a cyclonic circulation associated with a significant low at low-levels: The cyclonic circulation can be related to the formation of a mesoscale convective vortex on the northern line-end of the bow structure. The low is evident at 950 hPa around 11 UTC (Figure 9), becoming gradually more evident at 900 hPa (Figure 11), and it is more pronounced in WSM6-MYJ (Figures 9–11, left column) than in Thompson-YSU (Figures 9–11, right column). The cold pool deepens from 11 UTC to 13 UTC, more in the WSM6-MYJ simulation (Figure 10, left column) than in the Thompson-YSU one (Figure 10, right column). At 850 hPa; however, the cold pool feature, as deep as about 1500 m, is only pronounced in the WSM6-MYJ simulation (Figure 12, left column); it nearly disappears in the Thompson-YSU one (Figure 12, right column), since the cold pool is less deep in that simulation.

The stronger, deeper cold pool likely explains why the WSM6-MYJ simulation produces much stronger winds than the other simulations (e.g., Thompson-YSU) at the Liguria coastline locations examined. In addition, much stronger flow is present in the WSM6-MYJ run at 850 hPa (Figure 13, left panel) near and just behind the region of strong negative temperature tendencies, than in the Thompson-YSU one (Figure 13, right panel).

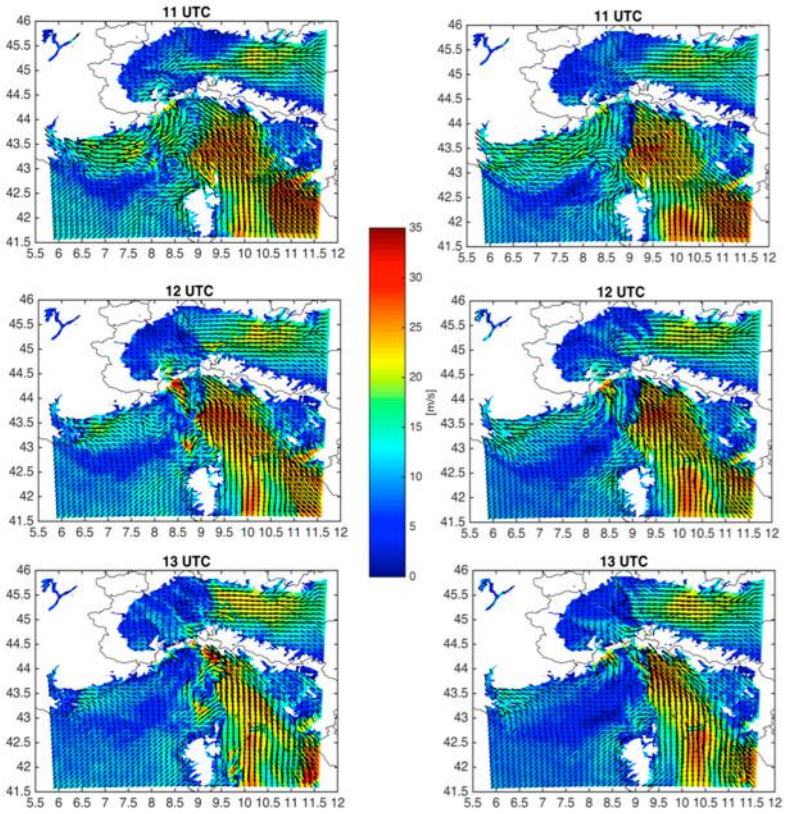

Figure 9. The 950 hPa wind field at 11, 12, and 13 UTC (WSM6-MYJ, left column; Thompson-YSU, right column).

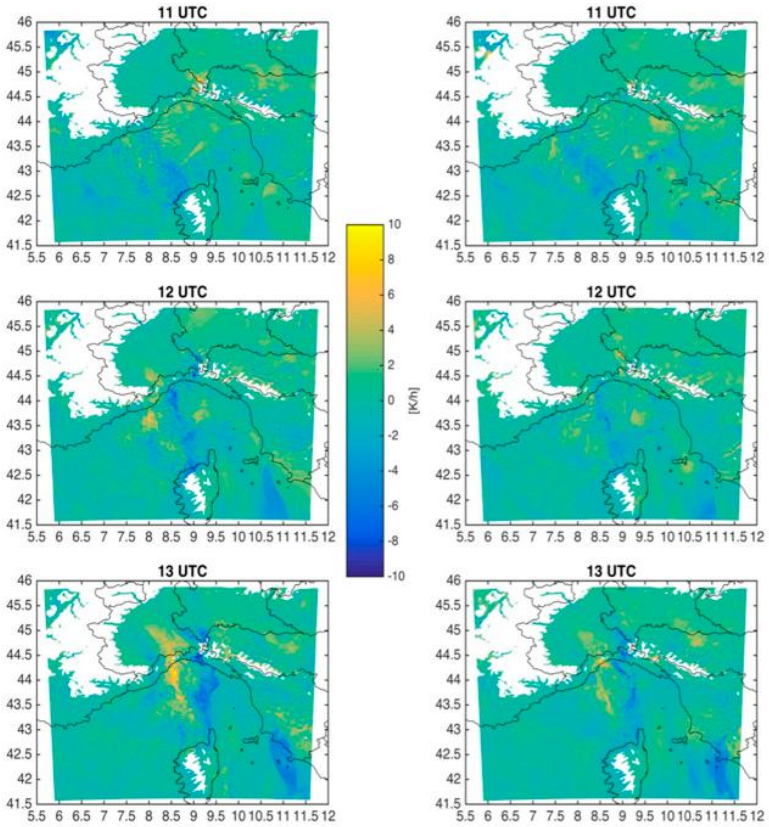

Figure 10. As in Figure 8 except for 900 hPa.

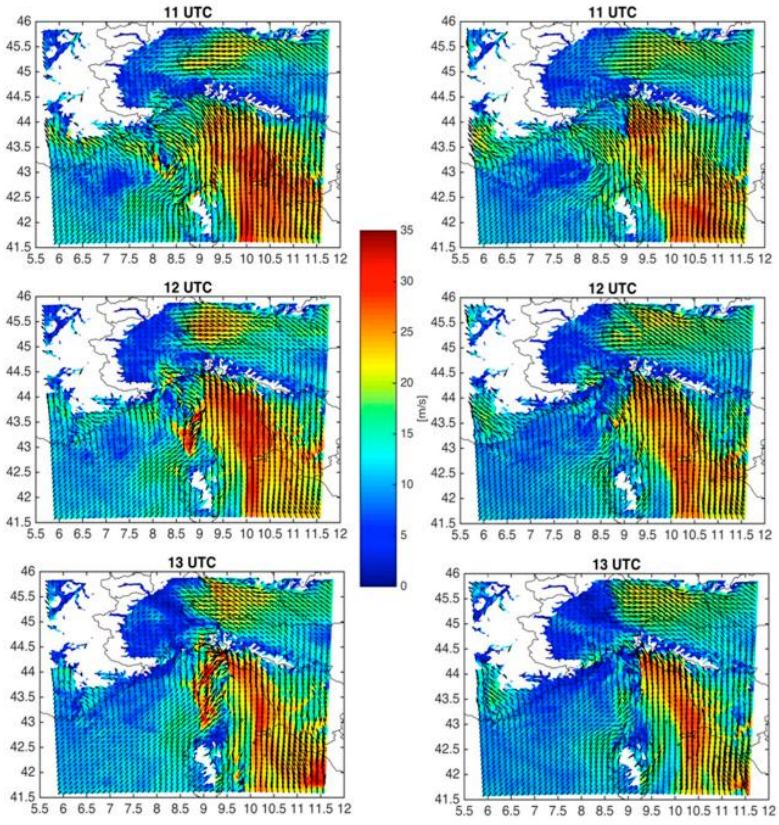

Figure 11. As in Figure 9 except for 900 hPa wind field.

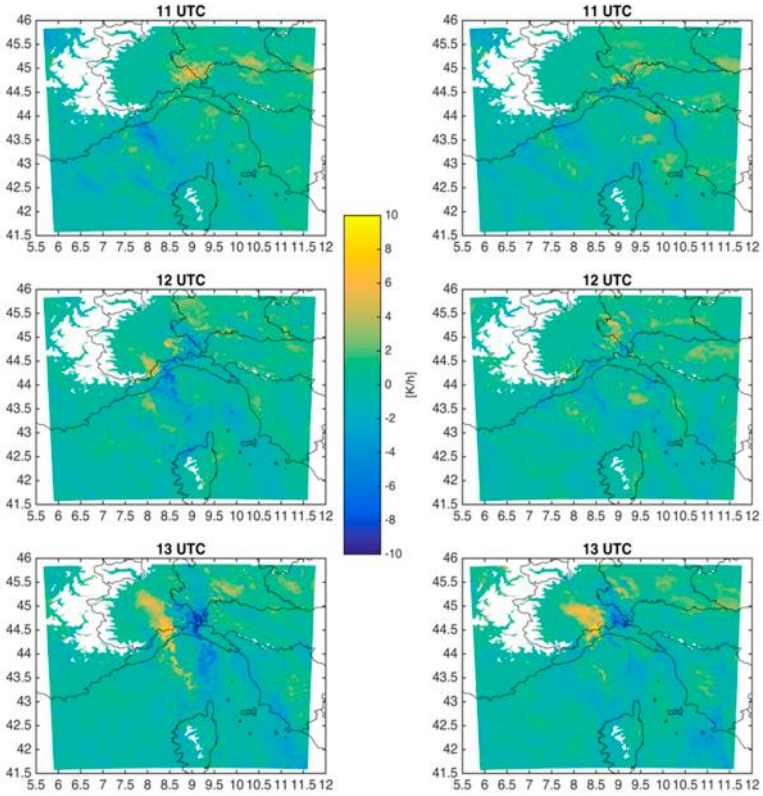

Figure 12. As in Figure 8 except for 850 hPa.

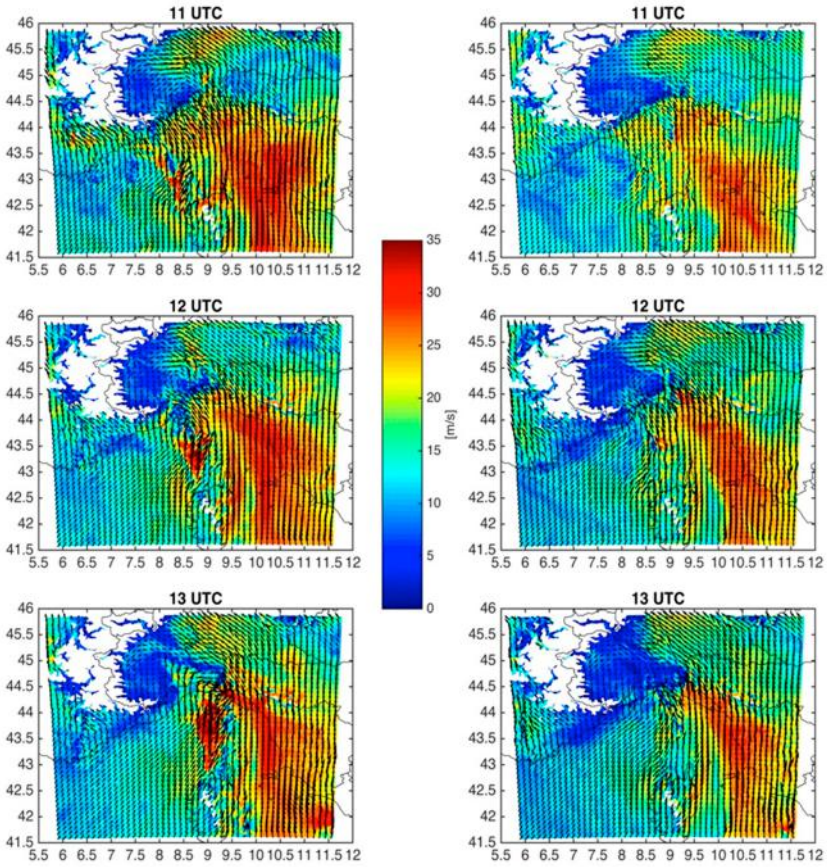

Figure 13. As in Figure 9 except for 850 hPa wind field.

Further insight into the modelling results can be gained by comparing the maximum 10 m wind speed predicted by WSM6-MYJ (Figure 14, first row, left panel) and Thompson-YSU (first row, right panel) over the period 1255–1300 UTC, just before the land impact. WSM6-MYJ produces a markedly more intense wind intensity (10 m/s higher than in Thompson-MYJ) with a very small displacement error over eastern Liguria. The higher intensity of the WSM6-MYJ wind gusts is due to a much more intense sea level pressure gradient near the Portofino promontory (Figure 14, second row), when compared with the Thompson-YSU patterns in the middle of the Ligurian sea. Additionally WSM6-MYJ exhibits intense lightning activity, as implied by the instantaneous lightning potential index (LPI) field [24,37,38], peaking at up to 500–600 J/kg (Figure 14, third row), much higher than the Thompson-YSU case with values of 150 to 200 J/kg, and in good agreement with the very intense lightning activity observed during this event (Figure 15). The LPI can be a good indicator of deep moist convective storms associated with very strong updrafts [24].

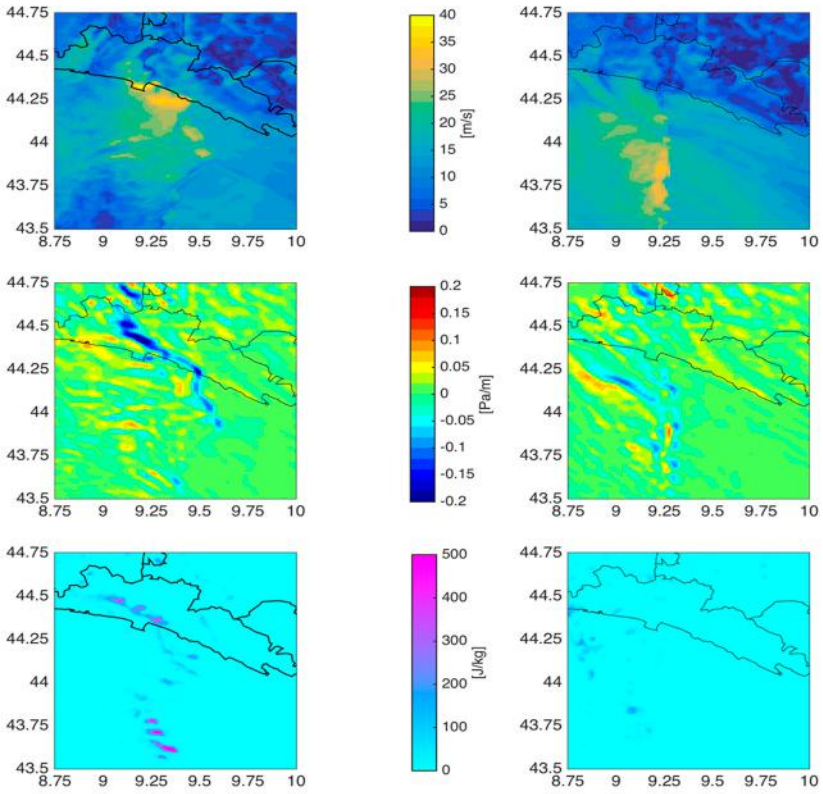

Figure 14. Maximum wind speed (m/s) 1255–13 UTC (first row, see color bar in the middle), sea level pressure gradient (Pa/m) at 13 UTC (second row, color bar in the middle), and LPI (J/kg) at 13 UTC (third row, color bar in the middle) for WSM6-MYJ (left column) and Thompson-YSU (right column).

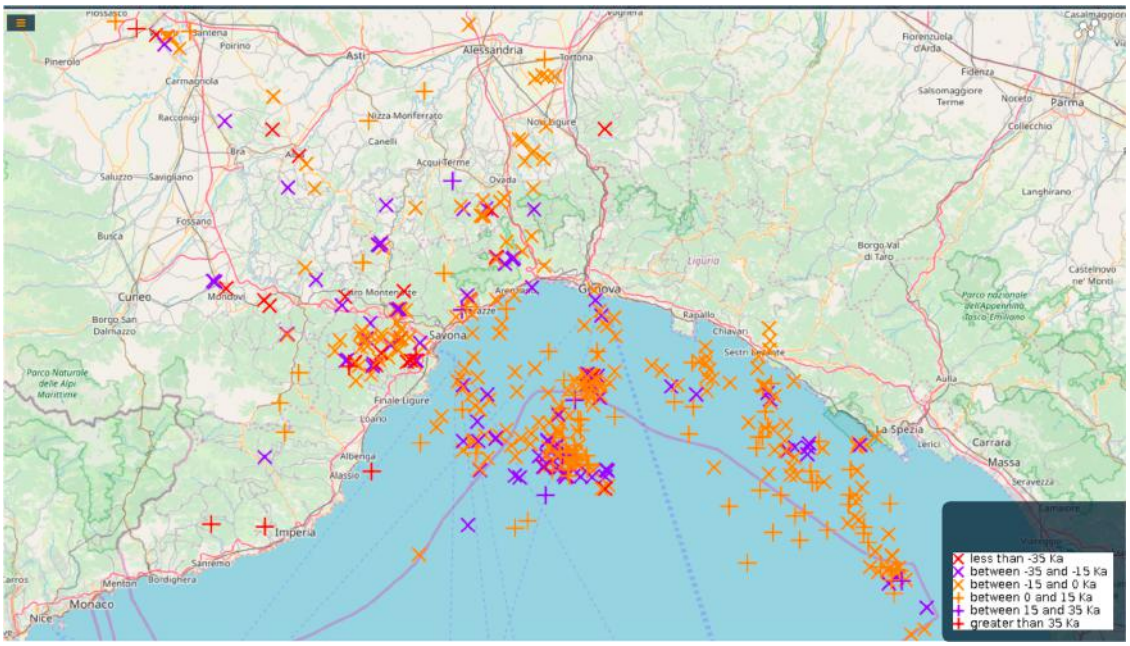

Figure 15. Location and intensity of the lightning strikes observed through the SFLOC (Sferic Location) method (1110–1115 UTC).

5. Conclusions

The macroburst episode that hit the Liguria region on 14 October 2016 was poorly predicted beforehand. Although a maximum level of alert was issued by ARPAL, it focused more on the possible development of intense and persistent convective storms producing significant accumulated rainfall, with some mention of possible winds around 20–25 m/s.

In this work, an observational and modelling study was performed, first identifying the main observed characteristics associated with this macroburst, and then presenting results of simulations using a small multi-physics high-resolution ensemble.

Some signs of downburst development (strong low-level winds and cold pool generation) were observed on the northwestern Corsica coast in the late morning, with a pressure increase and a temperature decrease. Reflectivity observations showed a possible bowing in the convective line rapidly propagating northeastward (about 150 km in 1 h and 45 min).

The macroburst event was simulated using four different microphysics parameterizations and two different planetary boundary layer parameterization schemes in the WRF-ARW at 1 km horizontal grid spacing. A comparison with observations indicates that the best performing simulation was WSM6-MYJ, with the worst being Thompson-YSU. The WSM6-MYJ produced a deeper cold pool, a greater pressure gradient, and a more intense maximum wind speed than Thompson-YSU. In addition, the WSM6-MYJ had the strongest wind speeds of all eight simulations, and the region of strong winds in the WSM6-MYJ run agreed well with the observed location of the strongest winds. Finally, the LPI for the WSM6-MYJ run provided a stronger signal for a strong convective event than that for the Thompson-YSU run.

In summary, the difficulty in forecasting this macroburst event is evidenced by the fact that so few ensemble members suggested the occurrence of damaging winds, even when very fine 1 km horizontal grid spacing was used in simulations initialized only about 12 h prior to the event. However, because one of the eight members performed well, its output helped to reveal the primary mechanisms for the macroburst, and this result suggests that high resolution ensembles using mixed physics may be a useful tool for improving the understanding of similar extreme events in the Mediterranean region in the future, if sufficient computer resources are available.

Nevertheless, in an operational forecasting situation, high-resolution ensembles may be too computationally expensive and may require too much time to run. Thus, further work should be done to explore other methods to extract information from smaller ensembles or those running with coarser grids, to provide better guidance for extreme events.

6. Data Availability

The data used in this study will be available via sftp server.

Author Contributions: Conceptualization, W.G.; Data curation, M.L.; Investigation, A.P., M.L. and B.T.; Methodology, M.M. and B.T.; Supervision, W.G.; Validation, A.P.; Writing—original draft, A.P.; Writing—review & editing, M.M. and W.G.

Funding: This research received no external funding.

Acknowledgments: We acknowledge the Italian Civil Protection Department for providing us with the Italian Weather Stations Network. We acknowledge Olivier Caumont (Météo-France/CNRS) for the provision of the Collobrieres radar data. Thanks are due to LRZ Supercomputing Centre, Garching, Germany, where the numerical simulations were performed on the SuperMUC Petascale System, Project-ID: pr62ve.

Conflicts of Interest: The authors declare no conflict of interest.

References

1. Fujita, T.T. Manual of downburst identification for project NIMROD. *SMRP Res. Pap.* **1978**, *156*, 104.
2. Fujita, T.T. Tornadoes and downbursts in the context of generalized planetary scales. *J. Atmos. Sci.* **1981**, *38*, 1511–1534. [CrossRef]
3. Fujita, T.T. Downbursts: Meteorological features and wind field characteristics. *J. Wind Eng. Ind. Aerodyn.* **1990**, *36*, 75–86. [CrossRef]
4. Fujita, T.T. The downburst. *SMRP* **1985**, *210*, 112.
5. Forbes, G.S.; Wakimoto, R.M. A concentrated outbreak of tornadoes, downbursts and microbursts, and implications regarding vortex classification. *Mon. Weather Rev.* **1983**, *111*, 220–236. [CrossRef]
6. Hjelmfelt, M.R. Structure and life cycle of microburst outflows observed in Colorado. *J. Appl. Meteorol.* **1988**, *27*, 900–927. [CrossRef]
7. Kessinger, C.J.; Parsons, D.B.; Wilson, J.W. Observations of a storm containing misocyclones, downbursts, and horizontal vortex circulations. *Mon. Weather Rev.* **1988**, *116*, 1959–1982. [CrossRef]
8. Wakimoto, R.M.; Bringi, V.N. Dual-polarization observations of microbursts associated with intense convection: The 20 July storm during the MIST project. *Mon. Weather Rev.* **1988**, *116*, 1521–1539. [CrossRef]
9. Kuster, C.M.; Heinselman, P.L.; Schuur, T.J. Rapid-update radar observations of downbursts occurring within an intense multicell thunderstorm on 14 June 2011. *Weather Forecast.* **2016**, *31*, 827–851. [CrossRef]
10. Mahale, V.N.; Zhang, G.; Xue, M. Characterization of the 14 June 2011 Norman, Oklahoma, downburst through dual-polarization radar observations and hydrometeor classification. *J. Appl. Meteorol. Climatol.* **2016**, *55*, 2635–2655. [CrossRef]
11. Pryor, K.L.; Johny, C.J.; Prasad, V.S. Evaluation of a convective downburst prediction application for India. In Proceedings of the Asia-Pacific Remote Sensing 2016, New Delhi, India, 4–7 April 2016; SPIE: Bellingham, WA, USA, 2016; Volume 9876, p. 987618.
12. Geerts, B. Estimating downburst-related maximum surface wind speeds by means of proximity soundings in New South Wales, Australia. *Weather Forecast.* **2001**, *16*, 261–269. [CrossRef]
13. Dotzek, N.; Friedrich, K. Downburst-producing thunderstorms in southern Germany: Radar analysis and predictability. *Atmos. Res.* **2009**, *93*, 457–473. [CrossRef]
14. Pistotnik, G.; Holzer, A.M.; Kaltenböck, R.; Tschannett, S. An F3 downburst in Austria—A case study with special focus on the importance of real-time site surveys. *Atmos. Res.* **2011**, *100*, 565–579. [CrossRef]
15. Púčik, T.; Francová, M.; Rýva, D.; Kolář, M.; Ronge, L. Forecasting challenges during the severe weather outbreak in Central Europe on 25 June 2008. *Atmos. Res.* **2011**, *100*, 680–704.
16. Burlando, M.; Romanić, D.; Solari, G.; Hangan, H.; Zhang, S. Field data analysis and weather scenario of a downburst event in Livorno, Italy, on 1 October 2012. *Mon. Weather Rev.* **2017**, *145*, 3507–3527. [CrossRef]

17. Orf, L.; Kantor, E.; Savory, E. Simulation of a downburst-producing thunderstorm using a very high-resolution three-dimensional cloud model. *J. Wind Eng. Ind. Aerodyn.* **2012**, *104*, 547–557. [CrossRef]
18. De Meutter, P.; Gerard, L.; Smet, G.; Hamid, K.; Hamdi, R.; Degrauwe, D.; Termonia, P. Predicting small-scale, short-lived downbursts: Case study with the NWP limited-area ALARO model for the Pukkelpop thunderstorm. *Mon. Weather Rev.* **2015**, *143*, 742–756. [CrossRef]
19. Tudurí, E.; Ramis, C. The environments of significant convective events in the western Mediterranean. *Weather Forecast.* **1997**, *12*, 294–306. [CrossRef]
20. Fiori, E.; Ferraris, L.; Molini, L.; Siccardi, F.; Kranzlmueller, D.; Parodi, A. Triggering and evolution of a deep convective system in the Mediterranean Sea: Modelling and observations at a very fine scale. *Q. J. R. Meteorol. Soc.* **2017**, *143*, 927–941. [CrossRef]
21. Gallus, W.A., Jr.; Parodi, A.; Maugeri, M. Possible impacts of a changing climate on intense Ligurian Sea rainfall events. *Int. J. Climatol.* **2018**, *38*, e323–e329. [CrossRef]
22. Skamarock, W.C. *Coauthors: A Description of the Advanced Research WRF Version 3*; NCAR Tech. Note; NCAR: Boulder, CO, USA, 2008; 113p. [CrossRef]
23. Fiori, E.; Comellas, A.; Molini, L.; Rebora, N.; Siccardi, F.; Gochis, D.J.; Tanelli, S.; Parodi, A. Analysis and hindcast simulations of an extreme rainfall event in the Mediterranean area: The Genoa 2011 case. *Atmos. Res.* **2014**, *138*, 13–29. [CrossRef]
24. Lagasio, M.; Parodi, A.; Procopio, R.; Rachidi, F.; Fiori, E. Lightning Potential Index performances in multimicrophysical cloud-resolving simulations of a back-building mesoscale convective system: The Genoa 2014 event. *J. Geophys. Res. Atmos.* **2017**, *122*, 4238–4257. [CrossRef]
25. Arakawa, A. The cumulus parameterization problem: Past, present, and future. *J. Clim.* **2004**, *17*, 2493–2525. [CrossRef]
26. Hong, S.Y.; Lim, J.O.J. The WRF single-moment 6-class microphysics scheme (WSM6). *J. Korean Meteorol. Soc.* **2006**, *42*, 129–151.
27. Thompson, G.; Field, P.R.; Rasmussen, R.M.; Hall, W.D. Explicit forecasts of winter precipitation using an improved bulk microphysics scheme. Part II: Implementation of a new snow parameterization. *Mon. Weather Rev.* **2008**, *136*, 5095–5115. [CrossRef]
28. Lim, K.S.S.; Hong, S.Y. Development of an effective double-moment cloud microphysics scheme with prognostic cloud condensation nuclei (CCN) for weather and climate models. *Mon. Weather Rev.* **2010**, *138*, 1587–1612. [CrossRef]
29. Morrison, H.; Thompson, G.; Tatarskii, V. Impact of cloud microphysics on the development of trailing stratiform precipitation in a simulated squall line: Comparison of one-and two-moment schemes. *Mon. Weather Rev.* **2009**, *137*, 991–1007. [CrossRef]
30. Hong, S.Y.; Noh, Y.; Dudhia, J. A new vertical diffusion package with an explicit treatment of entrainment processes. *Mon. Weather Rev.* **2006**, *134*, 2318–2341. [CrossRef]
31. Janjić, Z.I. The step-mountain eta coordinate model: Further developments of the convection, viscous sublayer, and turbulence closure schemes. *Mon. Weather Rev.* **1994**, *122*, 927–945. [CrossRef]
32. Parodi, A.; Tanelli, S. Influence of turbulence parameterizations on high-resolution numerical modeling of tropical convection observed during the TC4 field campaign. *J. Geophys. Res. Atmos.* **2010**, *115*. [CrossRef]
33. Iacono, M.J.; Delamere, J.S.; Mlawer, E.J.; Shephard, M.W.; Clough, S.A.; Collins, W.D. Radiative forcing by long-lived greenhouse gases: Calculations with the AER radiative transfer models. *J. Geophys. Res. Atmos.* **2008**, *113*. [CrossRef]
34. Copernicus Climate Change Service Climate Data Store (CDS). *ERA5: Fifth Generation of ECMWF Atmospheric Reanalyses of the Global Climate*; ECMWF: Reading, UK, 2017.
35. Smull, B.F.; Houze, R.A., Jr. A midlatitude squall line with a trailing region of stratiform rain: Radar and satellite observations. *Mon. Weather Rev.* **1985**, *113*, 117–133. [CrossRef]
36. Grim, J.A.; Rauber, R.M.; McFarquhar, G.M.; Jewett, B.F. Development and forcing of the rear inflow jet in a rapidly developing and decaying squall line during BAMEX. *Mon. Weather Rev.* **2009**, *137*, 1206–1229. [CrossRef]

37. Yair, Y.; Lynn, B.; Price, C.; Kotroni, V.; Lagouvardos, K.; Morin, E.; Llasat, M. Predicting lightning density in Mediterranean storms based on the WRF model dynamic and microphysical fields. In Proceedings of the AGU Fall Meeting, San Francisco, CA, USA, 15–19 December 2008.
38. Lynn, B.; Yair, Y. Prediction of lightning flash density with the WRF model. *Adv. Geosci.* **2010**, *23*, 11–16. [CrossRef]